GEOPHYSICS, VOL. 50, NO. 2 (FEBRUARY 1985); P. 207–213, 10 FIGS., 2 TABLES.

The influence of pore pressure and confining pressure on dynamic elastic properties of Berea sandstone

N. I. Christensen* and H. F. Wang‡

ABSTRACT

Compressional- and shear-wave velocities of water-saturated Berea sandstone have been measured as functions of confining and pore pressures to 2 kbar. The velocities, measured by the pulse transmission technique, were obtained at selected pressures for the purpose of evaluating the relative importance of confining pressure and pore pressure on elastic wave velocities and derived dynamic elastic constants. Changes in Berea sandstone velocities resulting from changes in confining pressure are not exactly canceled by equivalent changes in pore pressure. For properties that involve significant bulk compression (compressional-wave velocities and bulk modulus) an incremental change in pore pressure does not entirely cancel a similar change in confining pressure. On the other hand, it is shown that a pore pressure increment more than cancels an equivalent change in confining pressure for properties that depend significantly on rigidity (shear-wave velocity and Poisson's ratio). This behavior (as well as observed wave amplitudes) is related to the presence of high-compressibility clay that lines grains and pores within the quartz framework of the Berea sandstone.

INTRODUCTION

For many years, the influence of pore pressure on elastic wave velocities in sedimentary rocks has been of considerable interest to geophysicists. Wyllie et al. (1958) first demonstrated experimentally that compressional-wave velocities in Berea sandstone decrease with increasing pore pressure at constant confining pressures. Their data for water-saturated Berea sandstone showed that an increase in compressional-wave velocities produced by an increase in confining pressure (P_c) is canceled by an equal increase in pore pressure (P_p). Thus, velocity was found to be a constant value for a given differential pressure (Figure 1a). This was in direct conflict with an earlier theoretical analysis by Brandt (1955) for elastic wave velocity propagation in spheres as functions of pore and confining pressure, in which velocity was found to be dependent upon an effective pressure

$$P_e = P_c - nP_p \tag{1}$$

where n, termed the coefficient of internal deformation, is a number less than unity.

Shear-wave velocity measurements by Banthia et al. (1965) in three sandstones, including the Berea, and a chalk indicate that n is less than unity, in agreement with Brandt's theory. However, data obtained by King (1966) for the Berea sandstone showed that values of n were greater than unity for both compressional-wave velocities (Figure 1b) and shear-wave velocities (Figure 1c). Thus, even though both studies found $n \neq 0$, there is disagreement as to whether a greater (Banthia et al., 1965) or lesser (King, 1966) increase in pore pressure than confining pressure is required to maintain constant velocity in Berea sandstone.

In this study, we present compressional- and shear-wave velocities for Berea sandstone measured as functions of confining and pore pressure. We have taken advantage of new experimental design (Christensen, 1984) and higher voltage input pulses to produce rise times for the output signal and increased accuracies of the velocity measurements, which have been extended to pressures of 2 kbar. The relative importance of increases in confining and pore pressure is evaluated for Berea sandstone velocities as well as for the elastic moduli.

EXPERIMENTAL TECHNIQUE

The experimental assembly is similar to that described in detail in Christensen (1984). The sandstone sample is cylindrical, approximately 2.5 cm in diameter, and 3.3 cm in length. It is placed in a thin shell aluminum jacket containing longitudinal slots on its inside surface which are ported to the pore pressure pumping system. Transducers are placed directly on the ends of the sample. The sleeved sample assembly, transducers, and electrodes are jacketed with gum rubber tubing to prevent interaction of the confining and pore fluids. The pore pressure hydraulic system, which uses distilled water as the pore pres-

Manuscript received by the Editor June 26, 1984; revised manuscript received August 31, 1984.
*Department of Geosciences, Purdue University, West Lafayette, IN 47907.
‡Department of Geology and Geophysics, University of Wisconsin, Madison, WI 53706

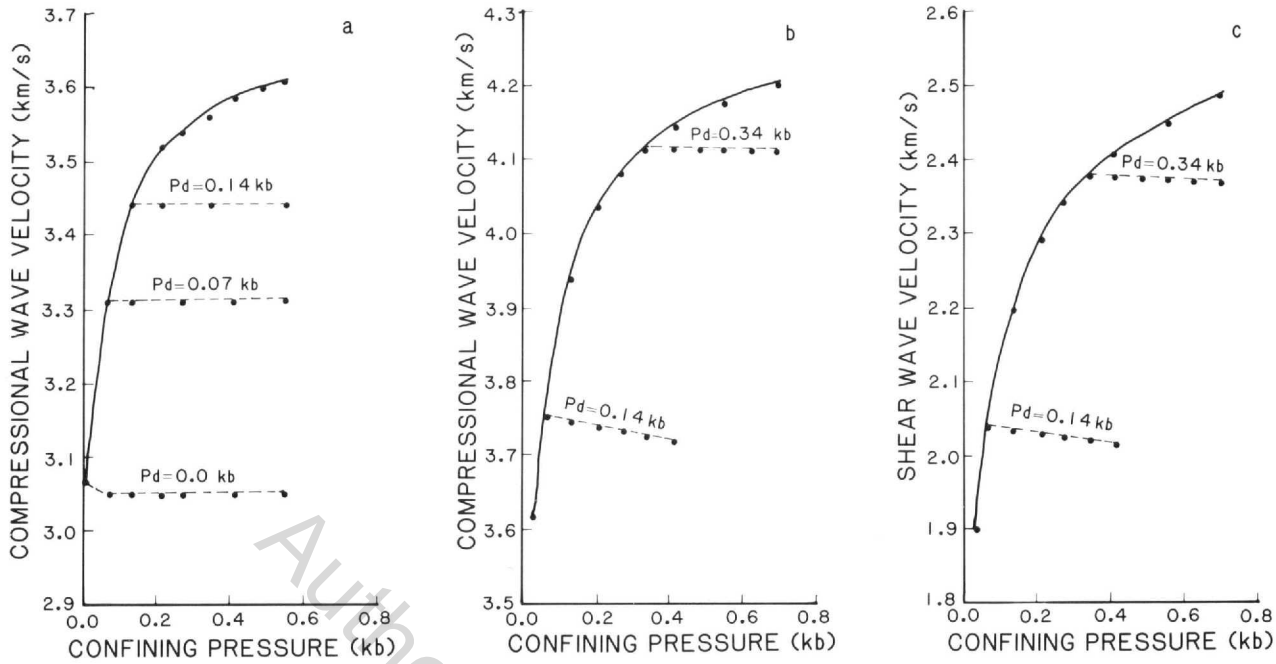

FIG. 1. Velocities in Berea sandstone as functions of confining and differential pressures. (a) Wyllie et al. (1958); (b) and (c) King (1966).

sure medium, is independent of the confining pressure hydraulic system. The confining pressure medium is hydraulic oil. Pressure is generated in both systems with hand pumps and measured with Heise bourdon gauges with accuracies of 0.1 percent to 2.5 kbar.

Velocities are obtained using a pulse transmission technique (Birch, 1960) in which measured traveltimes of elastic waves through the rock and sample length are used to calculate velocities. Lead-zirconate transducers are used for compressional-wave velocity measurements, whereas, for improved resolution, ac-cut quartz and lead-zirconate transducers generate and receive the shear waves, respectively. The sending transducers are driven by a rectangular pulse of approximately 400 V and 0.5 μs width. The elastic wave produced by the sending transducer is transmitted through the sample and detected by the receiving transducer. The resulting electrical output is amplified and displayed on one trace of a dual-trace oscilloscope. The wave train, even at very low differential pressures, shows a reasonable signal quality (Figure 2). Transit time of the elastic wave through the sandstone is measured by superimposing arrivals from the sample and a calibrated variable-length mercury delay line.

The velocity measurements (Table 1, Figures 3 and 4) are taken (1) along paths of increasing and decreasing confining pressure at atmospheric pore pressure, and (2) at constant differential pressure. The calibrated amplitudes of the first peak (Figure 2) of each wave arrival were also recorded at selected pressures and are summarized in Figure 5. For each constant differential pressure data set, the confining and corresponding pore pressures required to maintain constant differential pressure are varied at random. Pressures are maintained for an average of approximately 24 hours prior to each velocity measurement. Monitoring of velocity versus time after changing pressures indicates that equilibrium at each data point is reached in generally less than 12 hours. The repeatability of the velocity measurements is better than $\frac{1}{2}$ percent and the accuracy is 1 percent.

SAMPLE DESCRIPTION

A single core was used for both compressional- and shear-wave velocity measurements. Petrographic and SEM examinations of the trimmed core ends show that, in addition to quartz, clay clasts and clay cement are abundant (Figures 6 and 7). Estimated porosity from the thin section is 20 percent. Approximately 70 percent of the examined thin section consists of subangular quartz grains, many of which are in contact with one another forming a rigid framework. Lithic fragments, feldspar, and opaques are also present as clastic grains. The most abundant matrix material is clay ($\cong$10 percent), although carbonate and quartz are also common cementing materials.

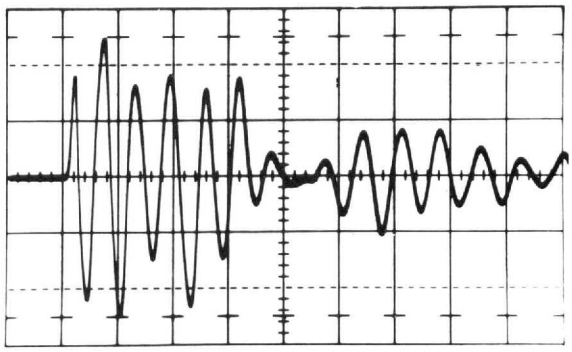

FIG. 2. Photograph of compressional-wave arrival at 1.200 kbar confining pressure and 1.195 kbar pore pressure.

Porosity of the sample used for the velocity measurements, as determined by comparison of the dry and water-saturated core weights, is 19.2 percent. The wet bulk density calculated from the weight and volume of the core is 2.253 g/cm^3.

VELOCITY DATA IN TERMS OF EFFECTIVE STRESS

The separate effects of confining pressure and pore pressure on the elastic wave velocities and derived dynamic elastic constants can be considered by using the concept of an effective pressure. Confining pressure P_c and pore pressure P_p are expected to have roughly equal, but opposite, effects on a bulk physical property. If the canceling effect of an increase in P_p exactly matches that of an increase in P_c, a physical property is a function of the single state variable $P_d = P_c - P_p$, where P_d is the differential pressure.

Empirical *n*

In general, an empirical factor n can be introduced to define the effective pressure $P_e = P_c - nP_p$ for cases where the pore

Table 1. Compressional wave velocities (V_p), shear wave velocities (V_s), and Poisson's ratios (σ) at various confining pressures (P_c) and pore pressures (P_p) for Berea sandstone.

P_c (kbar)	P_p (kbar)	V_p (km/s)	V_s (km/s)	V_p/V_s	σ
0	0	3.385	—	—	—
0.02	0	3.512	1.826	1.923	0.315
0.03	0	3.615	—	—	—
0.04	0	3.655	2.002	1.826	0.285
0.05	0	3.750	2.051	1.828	0.286
0.10	0	3.950	2.229	1.772	0.267
0.10	0.095	3.430	—	—	—
0.20	0	4.108	2.332	1.762	0.263
0.25	0	4.145	—	—	—
0.30	0	4.189	2.380	1.760	0.262
0.30	0.25	3.792	2.032	1.866	0.298
0.40	0	4.246	2.415	1.758	0.261
0.40	0.395	3.456	—	—	—
0.50	0	4.275	2.430	1.759	0.262
0.60	0	4.284	2.455	1.745	0.256
0.60	0.40	4.135	2.303	1.796	0.275
0.60	0.55	3.807	2.014	1.890	0.306
0.60	0.595	3.470	—	—	—
0.70	0	4.320	2.464	1.753	0.259
0.80	0	4.334	2.468	1.756	0.260
0.90	0	4.350	2.479	1.755	0.260
0.90	0.85	3.859	1.990	1.939	0.319
0.90	0.895	3.495	—	—	—
1.00	0	4.352	2.492	1.746	0.256
1.00	0.40	4.311	2.440	1.767	0.265
1.20	1.15	3.877	1.984	1.954	0.323
1.20	1.195	3.494	—	—	—
1.40	1.20	4.188	2.295	1.825	0.285
1.60	0	4.410	2.517	1.752	0.259
1.60	1.00	4.352	2.442	1.782	0.270
1.60	1.55	3.886	1.965	1.978	0.329
1.60	1.595	3.529	—	—	—
1.70	0.70	—	2.480	—	—
1.80	1.795	3.545	—	—	—
2.00	1.00	—	2.485	—	—
2.00	1.40	4.373	2.446	1.788	0.272
2.00	1.80	4.231	2.281	1.855	0.295
2.00	1.95	3.926	1.930	2.034	0.341
2.00	1.995	3.548	—	—	—

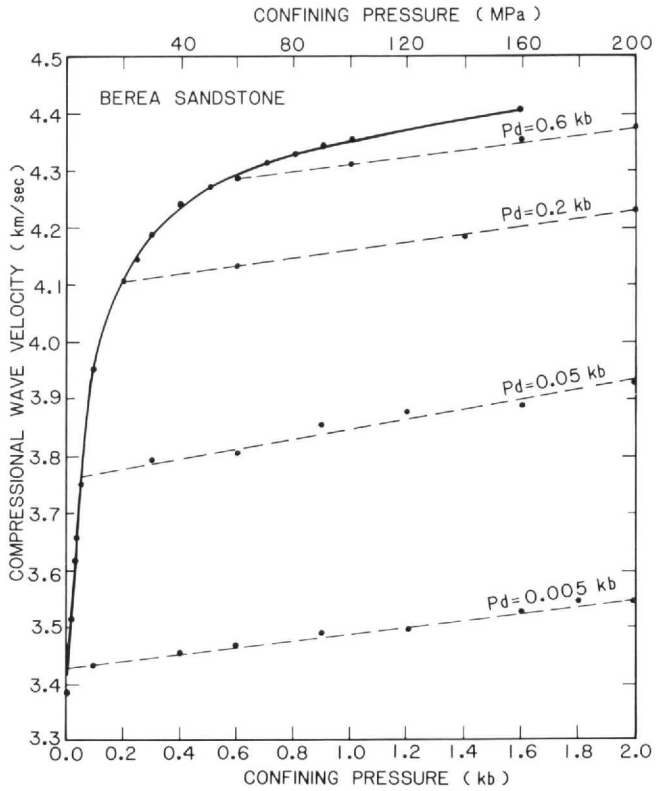

FIG. 3. Compressional-wave velocities as functions of confining pressure and differential pressure (P_d).

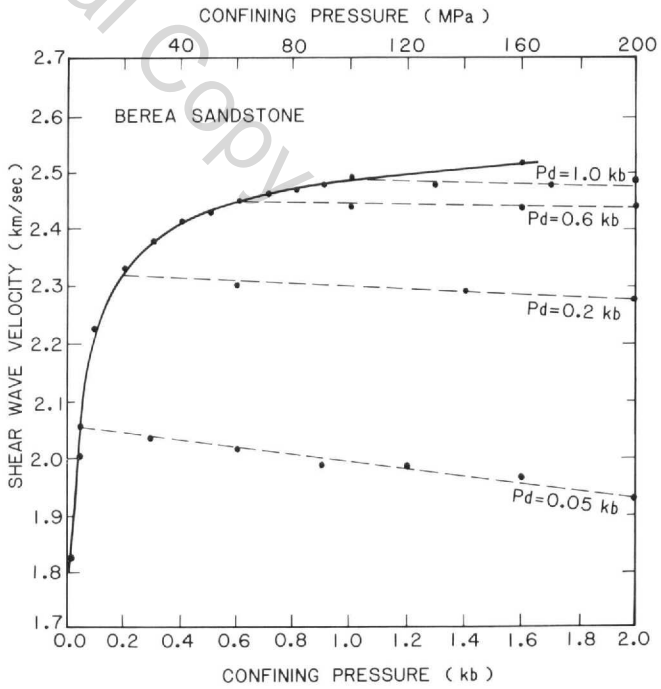

FIG. 4. Shear-wave velocities as functions of confining pressure and differential pressure (P_d).

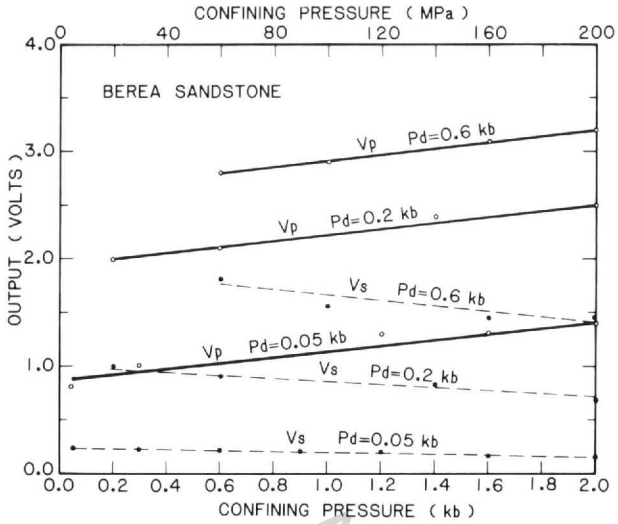

FIG. 5. Observed wave amplitudes in Berea sandstone at constant differential pressures. Open symbols for P amplitudes, solid symbols for S amplitudes.

pressure does not cancel confining pressure exactly. If n is a constant for all values of P_c and P_p, or equivalently, P_c and P_d, then the effective pressure combines the separate effects of P_c and P_d into a single state variable P_e. If n is itself a function of P_c or P_d, then an empirical value of n can be calculated from the expression (Todd and Simmons, 1972; Christensen, 1984)

$$n = 1 - \frac{(\partial Q/\partial P_p)_{P_d}}{(\partial Q/\partial P_d)_{P_p}} \tag{2}$$

where Q is any physical quantity. A value of n less than 1 implies that a pore pressure increment does not entirely cancel a confining pressure increment. A value of n greater than 1 implies that a pore pressure increment does more than cancel a confining pressure increment. For each physical property represented in Figures 3, 4, 8, and 9, a value of n can be calculated for any pair of values (P_c, P_d). These empirically obtained values are given in Table 2 for $P_c = P_d$, that is, along the curve $P_p = 0$. A contour of constant P_d is generally linear; the slopes $(\partial Q/\partial P_c)_{P_d}$ of the dashed lines were used for the $(\partial Q/\partial P_p)_{P_d}$ term because $\partial P_p = \partial P_c$ for constant P_d. The $(\partial Q/\partial P_d)_{P_p}$ term was approximated from the next differential pressure point along the $P_p = 0$ curve.

Table 2. Empirical values of n for $P_p = 0$.

		P_d (kbar)				
		0.005	0.05	0.2	0.6	1.0
Berea	V_p	0.99	0.93	0.89	0.84	—
	V_s	—	1.02	1.06	1.07	1.17
	K	—	0.89	0.78	—	0.50
	σ	—	1.07	—	—	—
Boise*	Bulk vol.	1.00	0.98	0.82	0.77	—

*Fatt, 1959

The most noteworthy feature of Table 2 is that the empirically derived values of n are less than 1 for properties that involve significant bulk compression (V_p and K) but are greater than 1 for properties that involve significant shear (V_s and σ).

Theoretical n

The theory of fluid-saturated porous materials leads to the conclusion that values of n for bulk volumetric deformation are given by

$$n = 1 - \frac{\beta_s}{\beta} \tag{3}$$

where β_s is the compressibility of the solid grains and β is the compressibility of the bulk material (Biot and Willis, 1957; Geertsma, 1957). Because the bulk compressibility decreases as a function of differential pressure, n also decreases as a function of differential pressure. We are not able to calculate the theoretical n based on the bulk modulus values in Table 2 because these represent dynamic values, not static ones as required by the theory. However, values for Boise sandstone are shown in Table 2 for comparison.

This theoretical n refers strictly to the effective pressure law for bulk volume and not to any other physical property. However, we might expect a similar effective pressure behavior for another physical property to the extent that it is sensitive to bulk volume. In this sense, the dynamic bulk modulus and compressional velocity show empirical n behavior similar to that of Boise sandstone. Shear velocity also is sensitive to bulk volume. Generally as pore space is reduced, the shear velocity increases; hence the shear velocity behavior with changes in both confining and pore pressure might be expected to be determined by their effects on the bulk volume. However, the opposite behavior of n for shear velocity in the Berea sandstone suggests that the framework rigidity is responding differently to changes of P_c and P_p than is the bulk volume.

MODEL FOR EFFECTIVE STRESS BEHAVIOR

A value of $n > 1$ was found by Zoback (1975), Zoback and Byerlee (1975), and Walls and Nur (1979) for permeability of Berea sandstone. Their conceptual model is that a low-compressibility quartz framework responds to confining pressure, whereas high-compressibility clayey pore linings respond to pore pressure. Our model for shear velocity behavior of Berea sandstone is similar. We utilize the idea of normal and tangential contact stiffnesses introduced by Digby (1981) and Winkler (1983). Clay cement between quartz grains is highly compressed and direct contact between quartz grains is established under an increase of confining pressure. A concomitant increase of pore pressure compresses clays which coat grains and fill pore space and are adjacent to the quartz-quartz contact. The net effect of equal increments of confining and pore pressure is to increase the stiffness in a direction normal to framework grain interfaces while decreasing the resistance to a tangential displacement. We show that this model allows framework rigidity to be reduced while the compressional velocity is still increased.

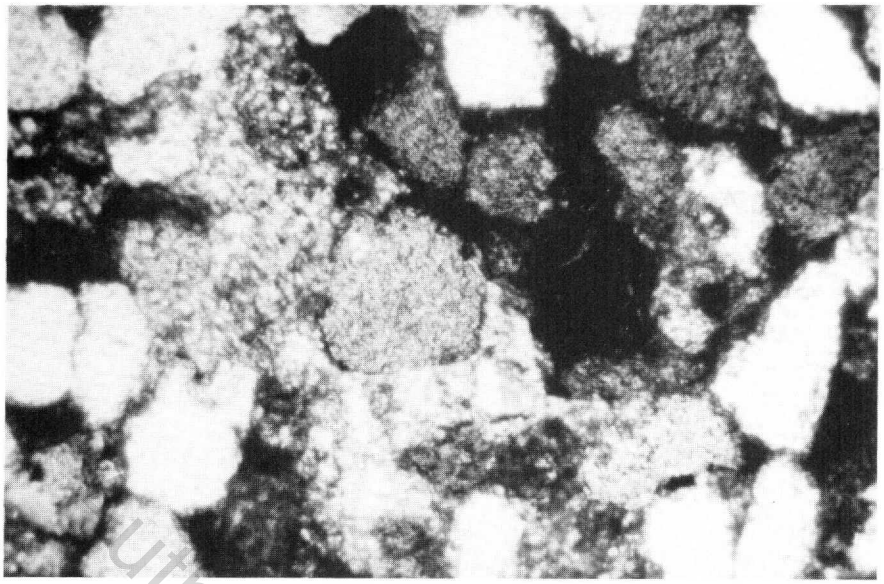

FIG. 6. Thin-section photograph of Berea sandstone showing quartz grains, clay clasts, and clay pore filling. Field of view is 1.0 × 1.5 mm.

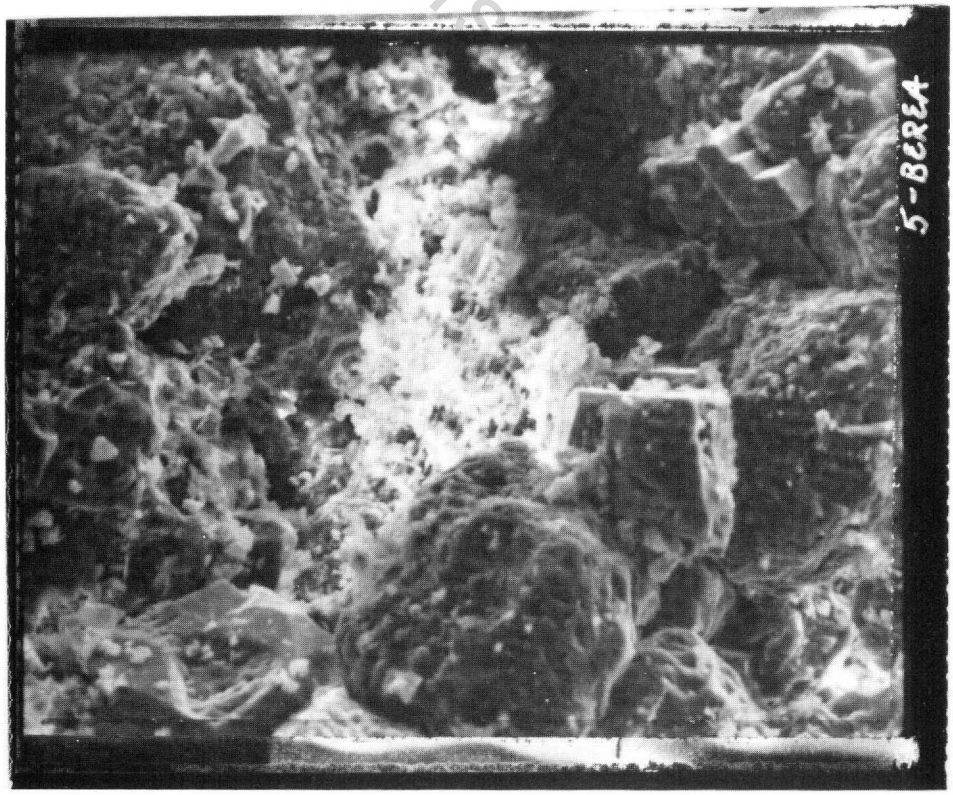

FIG. 7. SEM photograph of clay pore filling (light colored in center of photograph) between rounded quartz grains and angular feldspar and carbonate (300X).

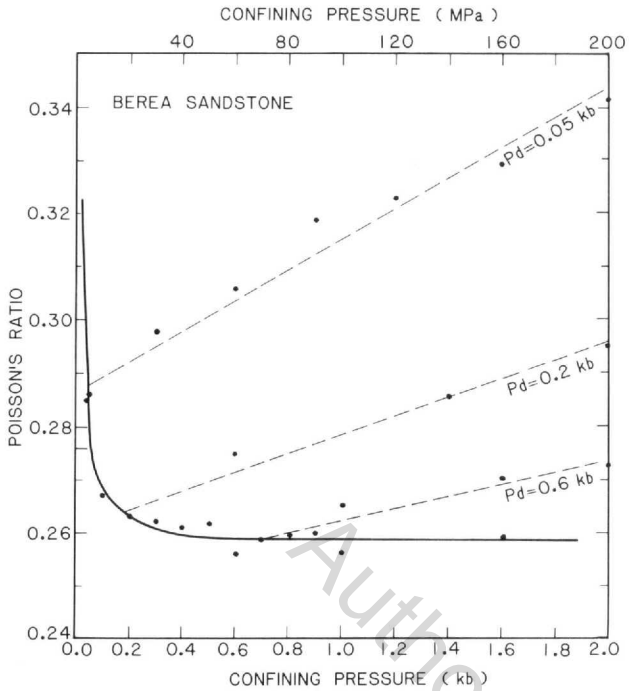

FIG. 8. Poisson's ratios calculated from V_p and V_s as functions of confining pressure and differential pressure (P_d).

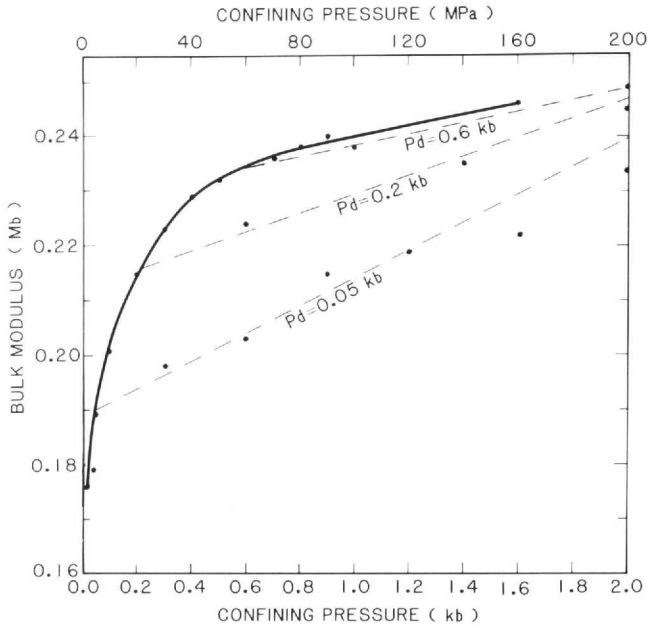

FIG. 9. Bulk moduli calculated from ρ, V_p, and V_s.

Our model is illustrated schematically for spherically shaped grains in Figure 10. The normal and tangential stiffnesses D_n and D_t, respectively, are defined by Digby [1981, equations (15) and (16)]:

$$D_n = dY/d\delta \tag{4}$$

and

$$D_t = dT/ds, \tag{5}$$

where Y is the normal force, δ is normal displacement, T is tangential force, and s is tangential displacement. Confining pressure increases D_n by forcing more framework contact between quartz grains. Pore pressure decreases D_t by decreasing the volume of the highly compressible clays. The dependence of V_p and V_s on D_n and D_t is given by Winkler [1983, equations (7) and (8)]:

$$V_p^2 = \frac{C}{20\pi R\rho}\{3D_n + 2D_t\} \tag{6}$$

$$V_s^2 = \frac{C}{20\pi R\rho}\{D_n + \tfrac{3}{2}D_t\}, \tag{7}$$

where $C = N(1-\phi)$, N = average number of contacts per grain, and ϕ = porosity, R is grain radius, and ρ is grain density. Four possibilities exist for the sign of ΔV_p and ΔV_s depending upon the magnitude and sign of ΔD_n and ΔD_t for equal increments of P_c and P_p. The result of the simple linear programming exercise is shown in Figure 11. For example, when the inequality

$$-\frac{3}{2} < \frac{\Delta D_t}{\Delta D_n} < -\frac{2}{3} \tag{8}$$

is satisfied, ΔV_p is greater than 0 while ΔV_s is less than 0, that is, $n < 1$ for V_p while $n > 1$ for V_s. The other three fields are labeled similarly in Figure 11.

Our model of elastic wave behavior in response to confining and pore pressure also applies to the observed wave amplitudes in Berea sandstone at constant differential pressure (Figure 5). The increase of normal contact stiffness is expected to increase wave amplitude for V_p, while the decrease of tangential contact stiffness is expected to decrease wave amplitude for V_s.

The shear-velocity data (Figure 4) suggest that the value of n approaches 1 for higher differential pressures. In terms of our model, higher differential pressures are associated with greater contact between quartz grains and lower compressibilities of clay linings near the contacts. Therefore, the ratio $\Delta D_n/\Delta P_c$ is expected to be smaller at higher differential pressures. Similarly, the ratio $\Delta D_t/\Delta P_p$ is expected to be less negative because of the greater clay stiffness near the contact. The shear-velocity data at high differential pressure indicate that for $\Delta P_c = \Delta P_p$, the location of the corresponding values of ΔD_t and ΔD_n in Figure 11 moves closer to the line $\Delta V_s = 0$ while remaining in the field described by $\Delta V_s < 0$ and $\Delta V_p > 0$.

Although there is no measure of contact stiffness changes with changes in confining pressure or pore pressure, the observed opposite dependencies of V_p and V_s at constant differential pressure are at least plausibly explained by the presence of clays in the Berea sandstone. Nonclayey sandstones which show $n < 1$ for both V_p and V_s would be represented in Figure 11 by different contact stiffness changes.

It should be emphasized that future velocity studies similar to the one presented here are highly desirable. Of importance will be measurements on sandstone samples with clay contents differing from the sample we have chosen.

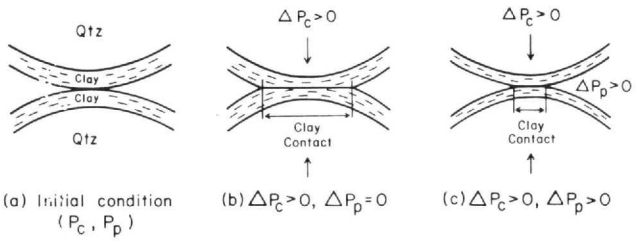

FIG. 10. Model of Berea sandstone response to equal changes in confining pressure and pore pressure.

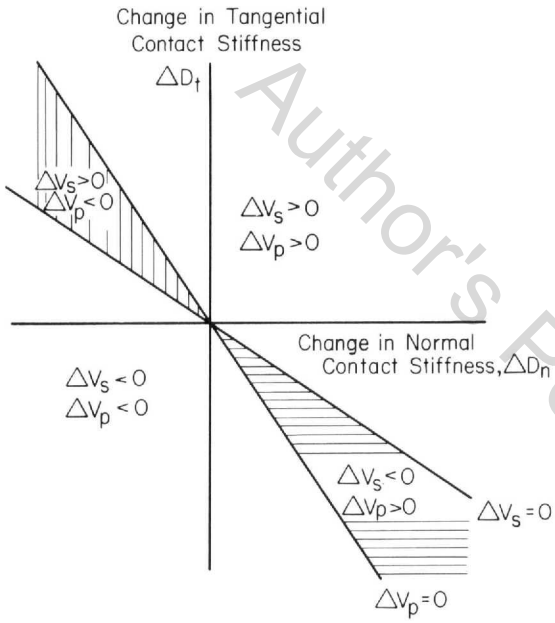

FIG. 11. Changes in V_p and V_s as functions of changes in contact stiffnesses D_n and D_t.

SUMMARY AND CONCLUSIONS

Our study and previous studies emphasize the importance of pore pressure on velocity behavior. V_p and V_s decrease by amounts up to 20 percent as pore pressure approaches the confining pressure. Poisson's ratio, as calculated from the velocities, is anomalously high (greater than 0.3) for high pore pressures, and thus serves as a sensitive indicator of the pore pressure environment.

The high-precision velocity data presented in Figures 3 and 4 show definitively that the effective stress behavior of V_p and V_s is different in Berea sandstone. For equal increments of increased confining and pore pressure, V_p is increased whereas V_s is decreased. A grain contact model, which incorporates the role of clays lining quartz grains and pores, provides the means for understanding the different effective stress behaviors. This model is supported by permeability measurements as functions of confining pressure and pore pressure (Zoback and Byerlee, 1975; Walls and Nur, 1979) for sandstones with differing clay contents.

ACKNOWLEDGMENTS

Support by the Office of Naval Research contract N-00014-80-C-0252 (Christensen) and Petroleum Research Fund grant no. 13115-AC2 (Wang) is gratefully acknowledged. B. Kowallis provided the SEM photographs.

REFERENCES

Banthia, B. S., King, M. S., and Fatt, I., 1965, Ultrasonic shear-wave velocities in rocks subjected to simulated overburden pressure and interval pore pressure: Geophysics, **30**, 117–121.
Biot, M. A., and Willis, D. G., 1957, The elastic coefficients of the theory of consolidation: J. Appl. Mech., **24**, 594–601.
Birch, F., 1960, The velocity of compressional waves in rocks to 10 kilobars, Part 1: J. Geophys. Res., **65**, 1083–1102.
Brandt, H., 1955, A study of the speed of sound in porous granular media: Trans. Am. Soc. Mech. Engrs., **22**, 479–486.
Christensen, N. I., 1984, Pore pressure and oceanic crustal seismic structure: Geophys. J. Roy. Astr. Soc., in press.
Digby, P. J., 1981, The effective elastic moduli of porous granular rocks: J. Appl. Mech., **48**, 803–808.
Fatt, I., 1959, The Biot-Willis elastic coefficients for sandstone: J. Appl. Mech., **26**, 296–301.
Geertsma, J., 1957, The effect of fluid pressure decline on volumetric changes of porous rocks: Soc. Petr. Eng., **210**, 331–340.
King, M. S., 1966, Wave velocities in rocks as a function of overburden pressure and pore fluid saturants: Geophysics, **31**, 56–73.
Todd, T. and Simmons, G., 1972, Effect of pore pressure on the velocity of compressional waves in low-porosity rocks: J. Geophys. Res., **77**, 3731–3743.
Walls, J. and Nur, A., 1979, Pore pressure and confining pressure dependence of permeability in sandstone: Presented at the 7th Formation evaluation symp. of the Canadian Well Logging Society, Calgary.
Winkler, K. W., 1983, Contact stiffness in granular porous materials: comparison between theory and experiment: Geophys. Res. Lett., **10**, 1073–1076.
Wyllie, M. R. J., Gregory, A. R., and Gardner, G. H., 1958, An experimental investigation of factors affecting elastic wave velocities in porous media: Geophysics, **23**, 459–493.
Zoback, M. D., 1975, High pressure deformation and fluid flow in sandstone, granite and granular materials: Ph.D. thesis, Stanford Univ.
Zoback, M. D., and Byerlee, J. D., 1975, Permeability and effective stress: Bull., Am. Assn. Petr. Geol., **59**, 154–158.